TRIUMF Experiment E614
Technical Note

A Comparison of Spectrometer Designs with and without Central Proportional Chambers

D.H. Wright, TRIUMF

1 August 1997

Abstract

Two designs for the central region of the E614 spectrometer were studied using Monte Carlo simulations of muons stopping and decaying near the target. One design relies on proportional chambers immediately upstream and downstream of the target to determine the stop location of the muons. The other design has no proportional chambers next to the target and relies solely on data from more distant drift chambers to reconstruct the muon decay (stop) location. Using the total muon depolarization $1-P_\mu$ to discriminate between the two designs, it was found that the design with proportional chambers next to the target came closer to meeting the precision requirements for the measurement of $P_\mu\xi$.

Prior to the MIG proposal [1] the design of the E614 spectrometer called for the aluminum target to be sandwiched between two pairs of CF_4 - ISO proportional chambers. The purpose of these chambers was to positively identify muons stopping in the target and distinguish them from muons stopping and depolarizing outside of the target. For several reasons, including ease of construction, reduction of multiple scattering and depolarizing mass, and target interchangeability, removal of these chambers was considered. For this to be feasible, it must be possible to reconstruct with sufficient position resolution the muon stopping location from the drift chamber hits of the incoming muon and decay positron tracks. Since depolarization of muons in the helium gaps is small it would only be necessary to guarantee that the muon did not stop in the innermost drift chamber pairs centered at $z = \pm 3.2$ cm.

No Proportional Chambers Adjacent to Target

This problem was studied using the baseline Monte Carlo spectrometer with no proportional chambers next to the target. A realistic beam of surface muons was introduced at $z = -67$ cm and allowed to propagate and decay in the spectrometer. Both the muon and positron tracks were reconstructed from drift chamber hits with 50 μm position uncertainty. Each track was reconstructed by taking the four drift chamber hits closest to the muon stop location and fitting these hits with a helix. The helix parameters used to start the fit were taken from the Monte Carlo position and direction of the particle at the drift chamber closest to the muon stop location. The point of closest approach of the positron track to

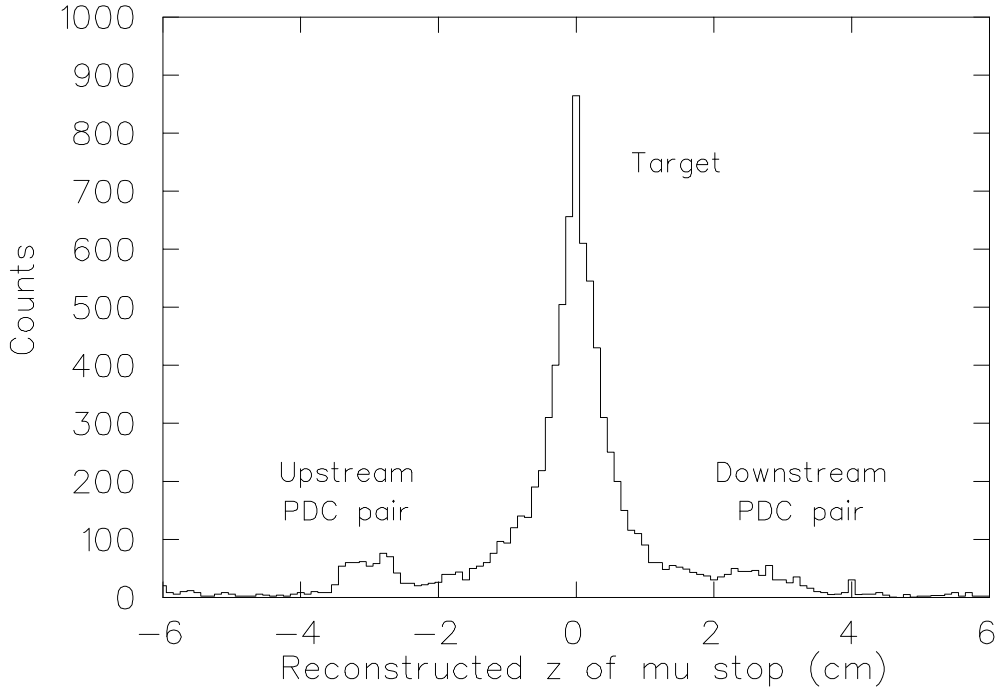

Figure 1: Reconstructed $z-$coordinate of muon stop location.

the muon track was then found and taken to be the muon stop location. A histogram of the $z-$coordinate of the calculated stop location is shown in Fig. 1.

The stopping location is not resolved as well as hoped, since the target distribution has a FWHM of 0.55 cm and long tails extending into the regions of the nearest upstream and downstream drift chamber pairs. The above distribution was the result of several methods used to improve the resolution, including iterating the calculation of the stop location using the previously determined stop location as a starting point.

The poor resolution is due almost entirely to the difficulty in fitting low energy muon tracks; the well-determined positron tracks contribute little to the width of the reconstructed distribution. By the time they approach the target the muons have so little energy that multiple scattering causes their tracks to deviate substantially from an ideal helix. The resulting fits are poor as indicated in Fig. 2.

The calculated intersections between muon and positron tracks are therefore also poor. The position error in z is given roughly by

$$\Delta z = \Delta xy / tan\theta \tag{1}$$

where θ is the angle of the positron track with respect to the z axis and Δxy is the distance of closest approach of the fitted muon track to the Monte Carlo stop. It is seen in Fig. 2 that the tail in the distribution of Δxy begins at about 0.9 cm. For a positron track at 10° the error in the reconstructed z of the muon stop could therefore be 5 cm or more. This explains the width of the reconstructed stopping distribution in Fig. 1.

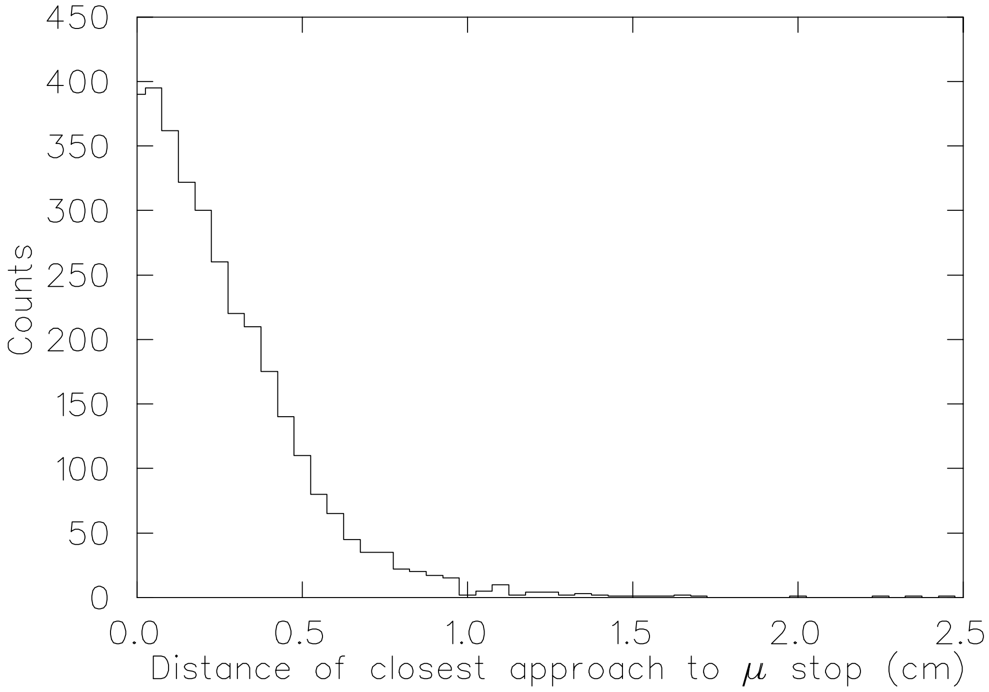

Figure 2: Distance of closest approach of fitted μ track to Monte Carlo stop location.

In order to reduce the probability that muons stopping in the upstream and downstream drift chambers had reconstructed stop locations near the target, a severe cut was placed on the reconstructed stop distribution of Fig. 1. It required that the reconstructed z coordinates of all stop locations be no more than 0.5 cm from the target, $z = 0$. Once this cut was imposed, the true (Monte Carlo) stop locations were histogrammed as shown in Fig. 3.

In addition to the above cut, only stops with z coordinates bewteen $\pm$ 2.81 cm were accepted. This condition was imposed because the muon stop location can be bounded, independent of track reconstruction, by observing which of the upstream and downstream drift chambers fired during an event. If the first two chambers upstream (PDC(-2), PDC(-1)) of the target fired and the first chamber downstream (PDC(+1)) of the target did not fire, the muon must have stopped between the active region of PDC(-1), ending at -2.81 cm, and the active region of PDC(+1), beginning at 2.81 cm. This region contains the target, two helium gaps, two buffer zones containing DME gas, and four mylar windows.

Using the distribution of stops in Fig. 3, the maximum muon depolarization was estimated by taking the stop-weighted average of the depolarization in all the materials in which the muon could stop between $\pm$ 2.81 cm :

$$\overline{1 - P_\mu} = \frac{N_{tgt}(1 - P_{\mu TGT}) + N_{He}(1 - P_{\mu He}) + N_{buf}(1 - P_{\mu DME}) + N_{My}(1 - P_{\mu My})}{N_{tgt} + N_{He} + N_{buf} + N_{My}}. \quad (2)$$

Here it has been assumed that the drift chambers are operating at 100% efficiency. The

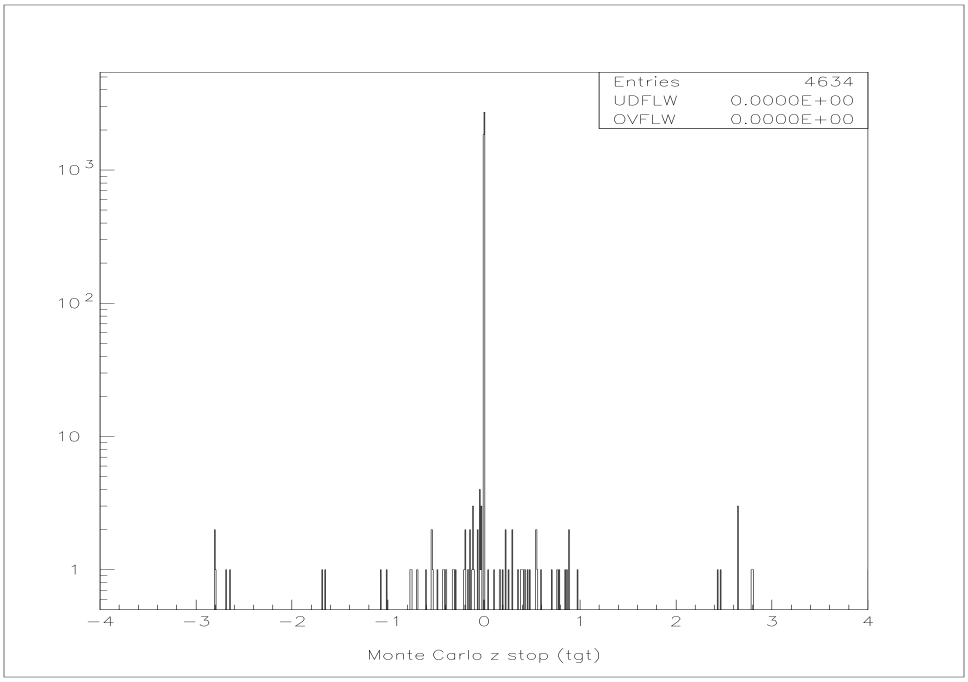

Figure 3: True (Monte Carlo) stop locations after the application of the $\pm$ 0.5 cm cut on the reconstructed stop locations.

effect of a small inefficiency is treated below. While it has not been measured, theoretical estimates of muon depolarization in DME give $P_{\mu DME} > 0.95$. For helium, $P_{\mu He} = 1.0$, but if a little DME should leak into the helium volume, the muon will have a greater affinity for the DME, thus increasing the depolarization. It was therefore assumed that $P_{\mu He} = 0.95$. For the target and mylar foils, the values $P_{\mu tgt} = 1.0$ and $P_{\mu My} = 0.0$, respectively, were taken.

Material	N_{stops}	$1 - P_\mu$
Al Target	4556	0.00
2 He gaps (upstream+downstream)	67	0.05
2 DME buffers (upstream+downstream)	4	0.05
4 Mylar foils (upstream+downstream)	7	1.00

Table 1. Number of Monte Carlo stops in the region $-2.81 < z < 2.81$ under the condition that the reconstructed z coordinate of the muon stop is within $\pm$ 0.5 cm of the target.

The number of Monte Carlo stops in the various volumes is given in Table 1. Using these values the average maximum depolarization was found to be

$$\overline{1 - P_\mu} = 2.3 \times 10^{-3}, \tag{3}$$

eight times larger than the desired precision of 3×10^{-4} in the Michel parameter $P_\mu \xi$. The final depolarization could be reduced further by tightening the cut on the reconstructed stop

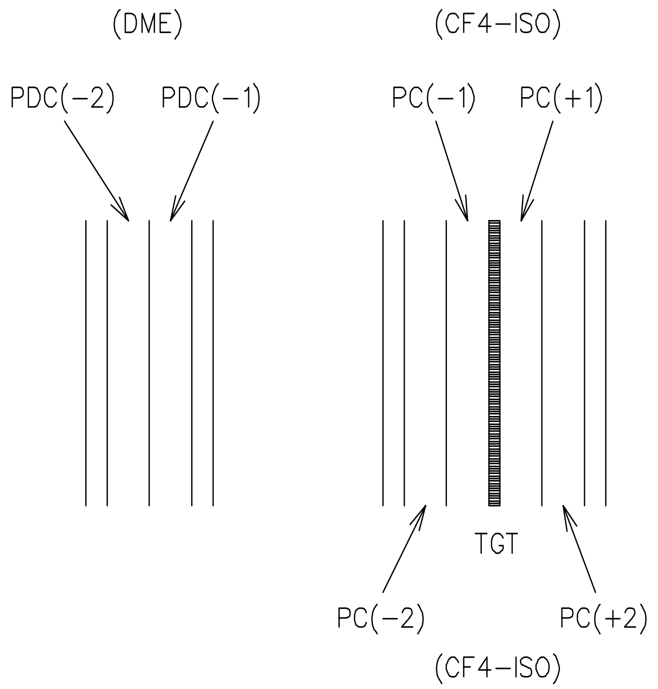

Figure 4: Central portion of spectrometer with proportional chambers (PCs) next to target and drift chamber pairs (PDCs) at ± 3.2 cm.

location. However, the current value was obtained with a sample of 20,000 Monte Carlo incident muons of which 4634 remain as good events. Tightening the cut further would reduce the overall event efficiency significantly.

The drift chamber pairs nearest the target were centered at ± 3.2 cm. In another Monte Carlo simulation, these chambers were moved to ± 5.2 cm in the hope that this would reduce the number of muons stopped in the drift chambers but reconstructed near the target. The effect was to reduce the total depolarization by a factor of two, still not low enough. This reduction factor was not as large as expected because the larger helium gap increased the lever arm for multiple scattering occurring in the chambers.

Proportional Chambers Adjacent to Target

Four proportional chambers were added to the baseline Monte Carlo, two immediately upstream of the target PC(-1,-2) and two immediately downstream PC(+1,+2) as shown in Fig. 4. These chambers were filled with CF_4/isobutane (80/20). The thickness of absorbers in front of the muon beam was reduced slightly from that in the previous Monte Carlo in order to maintain a flat stopping distribution in the aluminum target. All other beam and spectrometer parameters were unaltered. In this case, no tracking or vertex reconstruction was required since the condition PC(-2)·PC(-1)·$\overline{PC(+1)}$ was enough to locate the stop. However, muons satisfying this condition could stop anywhere in the gas volume of PC(-1)

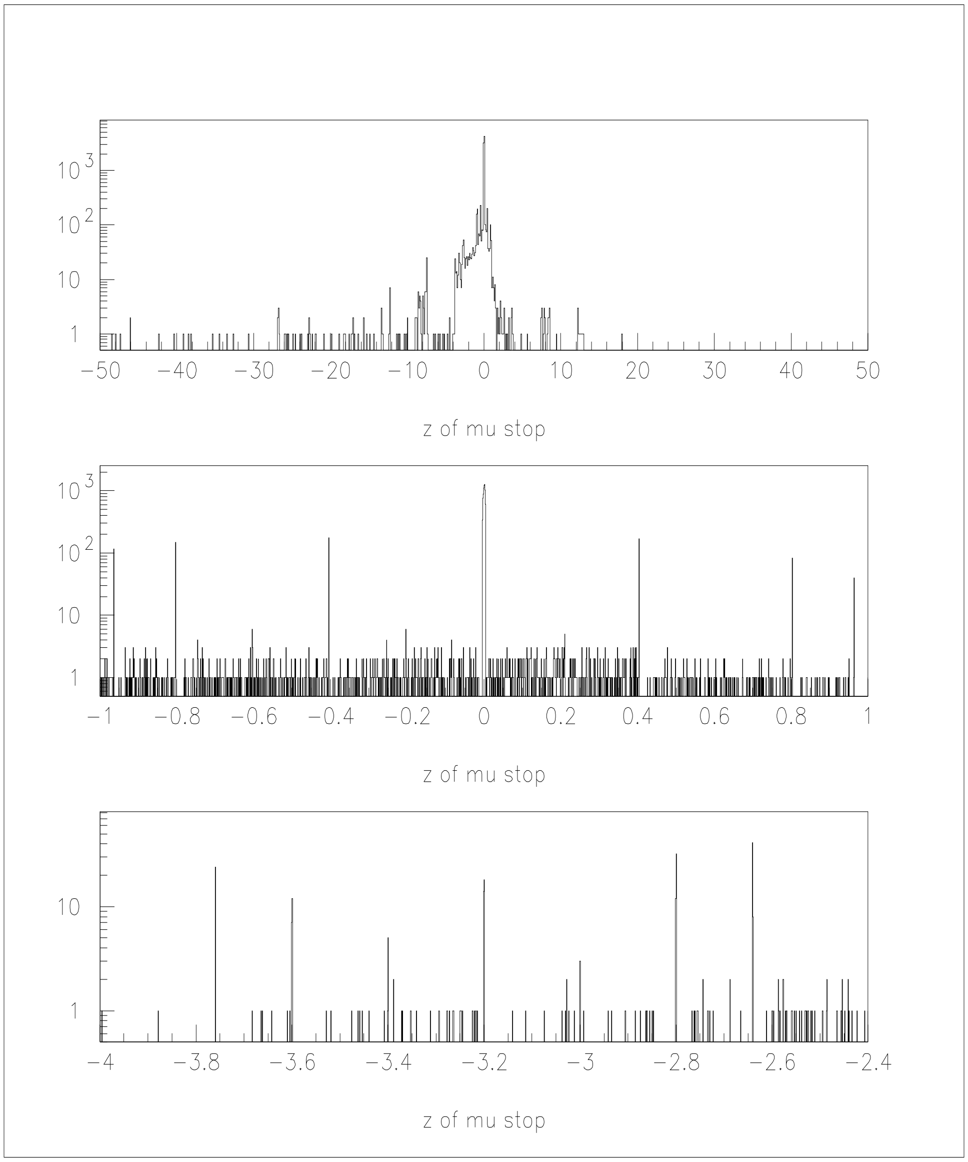

Figure 5: Muon stopping distribution with central PCs in place. Top: stopping distribution over entire spectrometer. Center: same spectrum as top, but for $-1.0 < z < 1.0$ cm. Bottom: same as top, but for $-4.0 < z < -2.4$ cm.

as well as in the target. Also, if the PCs are inefficient, a small fraction of stops in the gas of PC(+1) and the first downstream mylar foil would also satisy this condition.

The total depolarization was therefore obtained by counting the number of stops in each volume as shown in Fig. 5 (center) and taking the stop-weighted average of the depolarizations as before,

$$\overline{1-P_\mu} = \frac{N_{tgt}(1-P_{\mu TGT}) + N_{PC(-1)}(1-P_{\mu CF4}) + (1-\epsilon)[N_{PC(+1)}(1-P_{\mu CF4}) + N_{My}(1-P_{\mu My})]}{N_{tgt} + N_{PC(-1)} + (1-\epsilon)[N_{PC(+1)} + N_{My}]}. \tag{4}$$

Here $1-\epsilon$ is the PC inefficiency, taken to be 0.999. For 10,000 incident muons the number of stops in each volume is given in Table 2 along with the appropriate depolarizations. A lower limit on the depolarization in CF_4/isobutane was measured to be 0.985 [2].

Material	N_{stops}	$1-P_\mu$
Al Target	7212	0.000
CF_4-ISO (PC(-1))	269	0.015
CF_4-ISO (PC(+1))	338	0.015
1st Mylar foil downstream	172	1.000

Table 2. Number of Monte Carlo stops in the region $-0.4 < z < 0.4$.

For reference, Fig. 5 (bottom) shows the muon stopping distribution at the location of the first PDC pair upstream of the target. Most of the stops occur in the mylar foils as shown by the five largest spikes in the distribution.

Using Eq. 4 and the values of Table 2, the total muon depolarization for this spectrometer option was found to be

$$\overline{1-P_\mu} = 5.6 \times 10^{-4}. \tag{5}$$

This value, while four times better than the no-PC option, still needs improvement if the precision of 3×10^{-4} for $P_\mu\xi$ is to be reached. This could be achieved by a better measurement of the lower limit on the depolarization of muons in CF_4/ISO, which can be made during calibration runs or data taking. It could also be improved by removing more absorber from the muon beam, thus causing fewer muons to stop in PC(-1). At the same time more muons would stop in the gas of PC(+1), requiring good chamber efficiency to reject them. In this case the stopping distribution in the aluminum target would no longer be flat.

In conclusion, the spectrometer design with central proportional chambers comes much closer to the desired precison for E614. This design is also more efficient, keeping 72% of muon decay events, as opposed to 23% for the no-PC option.

References

[1] E614 collaboration Major Installation Grant proposal (1996).

[2] V. Selivanov, private communication, (1997).